scientific reports

Check for updates

OPEN

Reaction kinetics and molecular characterization of the compounds formed by photosensitized degradation of the plastic additive bisphenol A in the atmospheric aqueous phase

Yiting Wang[1], Qingxin Deng[2,3,5,6], Yiqun Wang[2,3,5,6], Pan Li[2,3,5,6], Biao Jin[2,3,5], Jiangping Liu[7], Peng Cheng[8], Marcello Brigante[8], Dario D'Antuono[9], Luca Carena[9], Hui Chen[1]✉, Davide Vione[9]✉ & Sasho Gligorovski[2,3,4,5]✉

Bisphenol A (BPA, 4,4'-(propane-2,2-diyl)diphenol) is a common plasticizer that is very widespread in the environment and is also found at significant concentrations in the global oceans, due to contamination by plastics. Here we show that triplet sensitization is an important degradation pathway for BPA in natural surface waters, which could prevail if the water dissolved organic carbon is above 2–3 $mg_C\ L^{-1}$. Bromide levels as per seawater conditions have the potential to slow down BPA photodegradation, a phenomenon that could not be offset by reaction of BPA with $Br_2^{\bullet-}$ (second-order reaction rate constant of $(2.54 \pm 0.09) \times 10^8\ M^{-1}\ s^{-1}$). Ultra-high resolution mass spectrometry revealed that the presence of inorganic salts (NaCl and NaBr) markedly increased the complexity of the observed CHO product compounds formed upon photosensitized degradation of BPA. The obtained results suggest that bisphenols can be efficiently removed by photosensitized reactions and generate higher number of oligomers and polyaromatic compounds in the sea surface and liquid water of marine aerosols compared to freshwaters and/or dilute cloud-water. Considering that polyaromatic compounds absorb solar actinic radiation, these results suggest that inorganic salts could significantly affect the photosensitized degradation of bisphenols and consequently influence the light-absorbing properties of marine aerosols and, ultimately, the Earth's radiative balance.

Keywords Photochemistry, Bisphenols, Aromatic compounds, Sea surface, Aerosols, Clouds

Microplastics are emerging environmental pollutants which represent a serious threat for the world's oceans[1]. It has been estimated that about 10% of the yearly production of plastic materials end up in the oceans, which amount to ca. 37 million tons[2]. The chemical additives of plastics can leach into seawater and accumulate at the sea surface microlayer (SML). Among plastic additives, bisphenols are toxic compounds widely used to form

[1]Key Laboratory of Organic Compound Pollution Control Engineering, School of Environmental and Chemical Engineering, Shanghai University, Shanghai 200444, China. [2]State Key Laboratory of Organic Geochemistry and Guangdong Provincial Key Laboratory of Environmental Protection and Resources Utilization, Guangzhou Institute of Geochemistry, Chinese Academy of Sciences, Guangzhou 510640, China. [3]Guangdong-Hong Kong-Macao Joint Laboratory for Environmental Pollution and Control, Guangzhou Institute of Geochemistry, Chinese Academy of Science, Guangzhou 510640, China. [4]University St. Kliment Ohridski Bitola, Boulevard 1st of May B.B, Bitola 7000, North Macedonia. [5]Chinese Academy of Science, Center for Excellence in Deep Earth Science, Guangzhou 510640, China. [6]University of Chinese Academy of Sciences, Beijing 101408, China. [7]Faculty of Environmental Science and Engineering, Kunming University of Science and Technology, Kunming 650500, China. [8]Institut de Chimie de Clermont-Ferrand, CNRS, Université Clermont Auvergne, 63000 Clermont-Ferrand, France. [9]Dipartimento di Chimica, Università di Torino, Via Pietro Giuria 5, 10125 Torino, Italy. ✉email: huichen@shu.edu.cn; davide.vione@unito.it; gligorovski@gig.ac.cn

hard plastic called polycarbonate. The biggest danger from bisphenols arises because they are unregulated and widely used in many countries of the world. Among these, bisphenol A (BPA, 4,4'-(propane-2,2-diyl)diphenol) is used in a broad variety of plastics as both containers and auxiliary materials in shampoos, body lotions, soaps, sunscreens, shaving creams, and detergents[3]. BPA is an organic contaminant that may exhibit estrogenic effects, increase the risk of certain cancers, and act as an endocrine disruptor[4]. It has been shown that BPA concentrations in oceanic surface waters range between 1 and 5 ng L^{-1}, while higher levels of up to 149 μg L^{-1} are reached in surface wastewater[5].

Some previous studies have focused on BPA degradation in terrestrial and aquatic environments by bacteria, fungi, and plants[6]. Although microbes can efficiently metabolize BPA in freshwater in about four days, this compound is not easily degraded in sea water where it can stay at the surface for more than a month[6,7]. It has been shown that BPA can be also transformed by ozone (O_3) oxidation reactions and by photosensitized reactions at the air-aqueous interface, including most notably the SML[8,9]. Zhan et al. (2006)[10] evaluated the effect of nitrate and ferric ions on the degradation of BPA induced by reactive oxygen species such as $^{\bullet}OH$, $^1O_2$, and H_2O_2 produced from excited humic substances. The presence of nitrate ions could promote the photodegradation of BPA[11]. It has been shown that humic acid and Fe^{3+} ions can enhance the photodegradation of BPA in simulated lake water containing algae[12].

The organic compounds with photosensitizing properties as a fraction of chromophoric dissolved organic matter (CDOM) are enriched at the SML or in aqueous aerosols[13]. Within the photosensitizers, aromatic carbonyls such as the 4-carboxybenzophenone (4-CB) may be produced during the oxidation of aromatic and phenolic compounds or by multiphase chemistry of oxygenated compounds in an aqueous phase containing ammonium sulfate[14,15]. They may also be formed as photolysis products of polycyclic aromatic hydrocarbons (PAHs)[14,16–19]. At the ocean surface or aqueous aerosols, the excited triplet states of aromatic carbonyls (e.g., ^{3}4-CB*) can be quenched efficiently by phenols, substituted phenols, as well as halide ions[20–23].

Recent study has evaluated the effect of NaCl, humic acid, and ^{3}4-CB* on the OH induced radical degradation of BPA in the aerosol phase[24]. The presence of 4-CB enhanced the photodegradation of BPA in the absence of $^{\bullet}OH$. No significant enhancements of photodegradation and OH induced loss of BPA, were observed when 4-CB was added to a mixture containing BPA and NaCl[24].

In particular, this study addresses the reaction kinetics between BPA and ^{3}4-CB* under conditions that may be significant for surface freshwaters, sea-water surface, and marine aerosols. A time-resolved spectroscopy technique was used to determine the second-order reaction rate constant of the dibromide radical anion ($Br_2^{\bullet-}$) with BPA in water. These data allow for an assessment of the photodegradation *vs.* biodegradation potential of BPA in freshwater vs. seawater.

To our best knowledge, ultra-high-resolution Fourier Transform Ion Cyclotron Resonance Mass Spectrometry (FT-ICR-MS) was used for the first time to perform a detailed analysis of the product-compound composition in the mass range of 100–1000 Da, following the photosensitized chemistry of BPA initiated by ^{3}4-CB* in the absence, and in the presence of sodium chloride (NaCl) and sodium bromide (NaBr).

Experimental

Irradiation experiments in photoreactor

A double-walled custom-built photoreactor made up of borosilicate glass, with a volume of 130 cm^3, was used to evaluate the photochemistry of 4-CB and 4-CB/BPA. The photoreactor is thermostated at 20 °C by thermostatic bath (LAUDA ECO RE 630 GECO, Germany).

Fresh solutions of either BPA (1×10^{-5} M) (Sigma-Aldrich, 98.5%) or BPA + 4-CB (both at 1×10^{-5} M) were prepared in ultrapure water (18.2 MΩ cm, Millipore). When required by the experimental protocol, NaCl and NaBr were also added to obtain concentration values of 0.7 M and 1 mM, respectively. The pH value was set at 7, measured by a pH meter (ORION STAR A326, Thermo Scientific, USA), and the solution was magnetically stirred during irradiation. The latter was performed by a high-pressure Xenon lamp (500 W), in combination with a circulating water filter to remove infrared radiation and a cutoff filter that let UV–Vis radiation pass, which is relevant to the lower atmosphere (300 nm ≤ λ ≤ 700 nm). The lamp emission spectrum was measured with a calibrated spectroradiometer (Ocean Optics, USA), equipped with a linear-array CCD detector (see Supplementary Fig. S1).

At each scheduled irradiation time, aliquots of 1 mL were taken from the photoreactor and directly injected into:

(i) A high-performance liquid chromatograph coupled with a diode array detector (HPLC–DAD). The VWR-Hitachi Chromaster instrument was equipped with model 5160 quaternary pump for low-pressure gradients, 5260 autosampler (60 μL injection volume), and 5430 DAD detector. It mounted a LiChroCART RP-C18 column packed with LiChrospher 100 RP-18 (VWR International, Milan, Italy, 125 mm × 4 mm × 5 μm). Elution involved isocratic conditions with 50% methanol / 50% acidified water (H_3PO_4, pH 3), producing the following features (retention time, quantification wavelength): BPA (13.3 min, 275 nm), 4-CB (15.2 min, 258 nm).
(ii) A FT-ICR-MS instrument for the analysis of liquid-phase products (vide infra). Analyses were performed immediately after sampling, thereby avoiding sample storage.

Solid phase extraction (SPE)

The SPE procedure has been described in detail in our previous studies[25,26], so here only brief description is given. We performed SPE of aqueous samples following light irradiation experiments of 4-CB and 4-CB/BPA with inorganic salts (NaCl, NaBr). Prior to FT-ICR-MS analysis, aqueous samples were inserted into SPE cartridges (Oasis WAX, 150 mg, 6 cc, 30 μm, Waters, USA) to eliminate inorganic salts and concentrate the

analytes. The Oasis WAX is a polymeric reversed-phase, weak ion-exchange, mixed-mode sorbent that allows for retention and release of strongly acidic, acidic, and neutral compounds, matching well with the ESI^- mode to detect acidic (i.e., easily deprotonated) molecules. In contrast, other compounds such as for instance basic molecules (e.g. piperidine) may get lost with the applied SPE procedure[27–29].

Sample analysis using FT-ICR-MS

After the scheduled irradiation times sample aliquots were collected and, if SPE was not necessary, they were diluted 1:9 v:v with methanol (HPLC grade, Merck & Co., Germany) prior to analysis with solariX XR FT-ICR-MS (Bruker Daltonik GmbH, Bremen, Germany). The selected water-to-methanol ratio is common for analysis based on previous test experiments, and methanol was verified not to react with analytes in the samples. We carried out control analyses and deleted the peaks that were also found in blank samples (reactant and solvent). The solariX XR FT-ICR-MS instrument is equipped with a refrigerated, 9.4 T actively shielded superconducting magnet (Bruker Biospin, Wissembourg, France) and a Paracell analyzer cell. Samples were ionized by an electron spray ionization source (ESI) in the negative ion detection mode. The detection mass range was set to *m/z* 150–1000, while ion accumulation time was set to 0.65 s. A total of 64 continuous 4 M data FT-ICR transients were co-added to enhance the signal-to-noise ratio and dynamic range. The mass spectra were calibrated externally with arginine clusters in the negative ion mode, using a linear calibration. The final spectrum was internally recalibrated with typical O_2 class species peaks, using quadratic calibration in DataAnalysis 4.4 (Bruker Daltonics). A typical mass-resolving power (m/Δm 50%, in which Δm50% is the magnitude of the mass spectral peak full width at half-maximum peak height) > 450,000 was achieved at *m/z* 319, with < 0.3 ppm absolute mass error. The details of data processing have been described previously[30,31].

Custom software was used to calculate all mathematically possible formulas for all ions with a signal-to-noise ratio above 10, using a mass tolerance of ± 0.6 ppm. The maximum number of atoms for the formula calculator was set to: 30 ^{12}C, 60 ^{1}H, 20 ^{16}O, 3 ^{14}N, 1 ^{32}S, 1 ^{13}C, 1 ^{18}O, and 1 ^{34}S[30,31].

The aromaticity equivalent (X_c) has been suggested for use to improve the identification and characterization of mono- and polyaromatic compounds[32–34]. Therefore, X_c values of organic compounds that contain C, H, O and, possibly, N and S in their chemical structures were calculated as follows:

$$X_C = \frac{2C + N - H - 2mO - 2nS}{DBE - mO - nS} + 1 \quad (1)$$

where *m* and *n* represent the fractions of oxygen and sulfur atoms involved in the π-bonds of a molecular structure[32] and DBE is the double-bond equivalent. In our calculations the values of *m* and *n* were set to 0.5, because ESI^- is most sensitive to compounds that contain carboxylic functional groups[33].

Laser flash photolysis experiments

A time-resolved spectroscopy apparatus was used to measure the second-order reaction rate constant of the dibromide radical anion ($Br_2^{\cdot-}$) with BPA in water. The experiments were carried out using the fourth harmonic (266 nm) of a Quanta Ray GCR 130-01 Nd:YAG laser system instrument and an energy of ~ 40 mJ/pulse. The experimental set-up has been described before[35]. $Br_2^{\cdot-}$ was generated from the photolysis of 10 mM H_2O_2 in the presence of 0.1 M Br^-, as reported in Supplementary Fig. S2 where a transient absorption signal with a maximum around 350 nm was observed. The decay of the signal monitored at λ = 350 nm (see Supplementary Fig. S2) was fitted with an exponential equation that yields the pseudo-first order decay constant (*k*', s^{-1}). The second order rate constant (M^{-1} s^{-1}) was then calculated from the slope of the linear correlation between *k*' and BPA concentration (varied from 0 to 0.5 mM) (see Supplementary Fig. S2). The error was calculated as ± σ, obtained from the scattering of the experimental data around the fit line.

Phototransformation kinetics of BPA

BPA underwent quite slow direct photolysis under the simulated sunlight irradiation, and considerably faster sensitized degradation in the presence of light-excited 4-CB (4-CB*). The overall reaction scheme is as follows (ISC = inter-system crossing; IC = internal conversion)[36]

$$4\text{-}\,\mathrm{CB} - (\mathrm{hv}) \rightarrow^1 4 - \mathrm{CB}* - (\mathrm{ISC}) \rightarrow^3 4\text{-}\,\mathrm{CB}* \quad (2)$$

$$^3 4\text{-}\,\mathrm{CB}* - (\mathrm{IC}) \rightarrow 4\text{-}\,\mathrm{CB} \quad (3)$$

$$^3 4\text{-}\,\mathrm{CB}* + \mathrm{O_2} \rightarrow 4\text{-}\,\mathrm{CB} + \mathrm{O_2}\left(^1\mathrm{O_2}\right) \quad (4)$$

$$\mathrm{BPA} +^3 4\text{-}\,\mathrm{CB}* \rightarrow \mathrm{BPA}^{\cdot+} + 4\text{-}\,\mathrm{CB}^{\cdot-} \quad (5)$$

$$4 - \mathrm{CB}^{\cdot-} + \mathrm{O_2} \rightarrow 4 - \mathrm{CB} + \mathrm{O_2^{\cdot-}} \quad (6)$$

$$\mathrm{BPA}^{\cdot+} \rightarrow \mathrm{Products} \quad (7)$$

$$\mathrm{BPA} +^1 \mathrm{O_2} \rightarrow \mathrm{Products}' \quad (8)$$

4-CB is known to have ISC yield around unity[37]. Note that reaction between triplet states and O_2 might yield either $^1O_2$, or ground-state (triplet) O_2. The $^1O_2$ yield in such processes is often around 50% (46% in the case of

^{3}4-CB*)[36,38]. Also note that $O_2^{\bullet-}$ formed in (Eq. 6) would disproportionate to H_2O_2, the photolysis of which yields $^\bullet$OH[39]. However, the role played by the limited amount of $^\bullet$OH thus formed is usually minor to insignificant if the substrate (BPA in this case) undergoes significant triplet sensitization, and can only be highlighted in the presence of hardly oxidized compounds[40].

Assuming the following[41]: (i) $P_a^{BPA} = \int_\lambda p^\circ(\lambda)[1 - 10^{-A_{BPA}(\lambda)}]\, d\lambda$ as the photon flux absorbed by BPA alone, where $p^\circ(\lambda)$ is the spectral photon flux density of lamp radiation and $A_{BPA}(\lambda)$ the absorbance of BPA in the irradiated solution; (ii) $P_a'^{BPA} = \int_\lambda p^\circ(\lambda)\frac{A_{BPA}(\lambda)}{A_{BPA}(\lambda)+A_{4-CB}(\lambda)}[1 - 10^{-A_{BPA}(\lambda)-A_{4-CB}(\lambda)}]\, d\lambda$ as the photon flux absorbed by BPA in the presence of 4-CB, where $A_{4\text{-CB}}(\lambda)$ is the absorbance of 4-CB in the irradiated solution; (iii) R'_{BPA} as the (measured) direct photolysis rate of BPA alone; (iv) $R''_{BPA} = R'_{BPA}\, P_a'^{BPA} / P_a^{BPA}$ as the direct photolysis rate of BPA in the presence of 4-CB that shades part of the incoming radiation, and (v) R_{BPA} as the measured rate of BPA degradation in the presence of 4-CB under simulated sunlight irradiation. In this framework, the rate of BPA photosensitization by 4-CB is $R_{BPA}^s = R_{BPA} - R''_{BPA}$. The plot of R_{BPA}^s *vs.* $[BPA]_o$ should give a straight line with slope Ξ and, when applying the steady-state approximation to ^{3}4-CB* and $^1O_2$ in Eqs. (1–7), the following expression for the second-order rate constant of the reaction (4) between BPA and ^{3}4-CB* is obtained[41]:

$$k_4 = k'_d \left(\frac{\Xi}{P_a'^{4-CB}} - \frac{0.68\, S_\Delta k_7}{k''} \right) \tag{9}$$

where[36]: $k'_d = 6 \times 10^5$ s^{-1} is the deactivation rate constant of ^{3}4-CB* in aerated solution; $P_a'^{4-CB} = \int_\lambda p^\circ(\lambda)\frac{A_{4-CB}(\lambda)}{A_{BPA}(\lambda)+A_{4-CB}(\lambda)}[1 - 10^{-A_{BPA}(\lambda)-A_{4-CB}(\lambda)}]\, d\lambda$ is the photon flux absorbed by 4-CB in solution in the presence of BPA; 0.68 is the fraction of ^{3}4-CB* that is quenched by O_2 (the remaining 32% undergoes internal conversion); $S_\Delta = 0.46$ is the $^1O_2$ yield of the reaction between ^{3}4-CB* and O_2; $k_7 = 3 \times 10^5$ M^{-1} s^{-1} is the second-order rate constant of the reaction between $^1O_2$ and BPA[42], and $k'' = 2.5 \times 10^5$ s^{-1} is the first-order rate constant of $^1O_2$ quenching in solution upon collision with water[43].

The primary oxidation reaction between a contaminant and excited triplet state(s) is not an end process, however, because back-reduction processes can sometimes occur[44]. The latter implies that the partially oxidized BPA transients (indicated as $BPA^{\bullet+}$ in reaction (4); they would typically be phenoxy radicals) might be reduced back to the parent BPA by anti-oxidant phenolic moieties occurring in dissolved organic matter (DOM). For this reason, phenol was here used as DOM antioxidant proxy and its effect was studied on the degradation kinetics of BPA by irradiated 4-CB. The following reactions would be involved in the kinetic model for back-reduction (PhOH = phenol; $PhO^\bullet$ = phenoxy radical)[45]

$$^3\text{4 - CB} * + \text{BPA} \rightarrow \text{4 - CB}^{\bullet-} + \text{BPA}^{\bullet+} \tag{10}$$

$$\text{BPA}^{\bullet+} + \text{PhOH} \rightarrow \text{BPA} + \text{PhO}^\bullet + \text{H}^+ \tag{11}$$

By applying the steady-state approximation to both ^{3}4-CB* and $BPA^{\bullet+}$ the following relationship between R_{BPA} and [PhOH] is obtained:

$$R_{\text{BPA}} = R^\circ_{\text{BPA}} \left(\frac{1}{1 + \frac{[\text{PhOH}]}{[\text{PhOH}]_{1/2}}} \right) \tag{12}$$

where R°_{BPA} is the initial BPA degradation rate in the absence of PhOH, and $[PhOH]_{½}$ is defined as the concentration of phenol that halves the BPA degradation rate because of the back-reduction process (i.e., when $[PhOH] = [PhOH]_{½}$, it is $R_{BPA} = ½\, R^\circ_{BPA}$).

It should be noted that, in some cases, not all the radical intermediates produced by triplet sensitization can undergo back-reduction. Thus, a different mathematical treatment is required to describe such systems[45,46].

Modeling of BPA photodegradation

BPA photodegradation kinetics was predicted by means of the software APEX (Aqueous Photochemistry of Environmentally-occurring Xenobiotics), which computes pseudo-first order rate constants due to photochemical reactions as a function of pollutant reactivity (absorption spectrum, direct photolysis quantum yield, second-order reaction rate constants with $^\bullet$OH, $CO_3^{\bullet-}$, $^1O_2$, and ^{3}CDOM*) and environmental features (sunlight irradiance, water chemistry, and water depth)[47]. BPA volatilization kinetics from surface waters was predicted by means of the EPI-SuiteTM package[48].

Results and discussion

Assessment of BPA photodegradation by ^{3}4-CB* in freshwater

The second-order rate constant ($k_4 = (4.6 \pm 0.2) \times 10^9$ M^{-1} s^{-1}) between BPA and ^{3}4-CB* is obtained from the linear plot of R_{BPA}^s *vs.* $[BPA]_o$ depicted in Supplementary Fig. S3. Note that the plot was linear up to 20 μM

BPA, above which concentration the scavenging of ^{3}4-CB* by BPA would become significant and a plateau trend would be reached. Furthermore, experiments in the presence of phenol allowed for the exclusion of significant back-reduction effects. It is also known that the direct photolysis of BPA is negligible in natural surface waters, thus significant reactions could take place with •OH ($k_{BPA,\cdot OH} = 1.0\times10^{10}$ M^{-1} s^{-1}), $CO_3^{\bullet-}$ ($k_{BPA,CO_3^{\bullet-}} = 2.8\times10^{8}$ M^{-1} s^{-1}), and $^1O_2$ ($k_{BPA,^1O_2} = 3\times10^{5}$ M^{-1} s^{-1})[42,49–51], plus ^{3}CDOM* for which reactivity (k_4) has been assessed here by using ^{3}4-CB* as proxy.

Figure 1 shows the modeled photodegradation pathways of BPA in typical freshwaters, suggesting that lifetimes would be in the days-week range. Moreover, •OH and $CO_3^{\bullet-}$ would prevail as pathways at low DOC (dissolved organic carbon), while ^{3}CDOM* would dominate high-DOC photodegradation. Photochemical BPA lifetimes would be relatively low (some days), thereby suggesting photodegradation as an important BPA removal process from surface waters. By comparison, EPI-Suite™ model calculations exclude significant BPA volatilization to the gas phase.

Reaction kinetics between BPA and $Br_2^{\bullet-}$

The laser flash photolysis measurements suggested that BPA is able to quench $Br_2^{\bullet-}$, with a calculated second-order rate constant of $(2.54\pm0.09)\times10^8$ M^{-1} s^{-1} and an intercept of linear fit of 2.0×10^5 s^{-1} (see Supplementary Fig. S2), corresponding to the pseudo-first order decay of $Br_2^{\bullet-}$ in water.

In brackish waters and saltwater, there would be effective scavenging of •OH by bromide[52,53], with high potential to suppress •OH-mediated processes and also to block the main $CO_3^{\bullet-}$ formation pathway (HCO_3^-/CO_3^{2-} oxidation by •OH)[54]. However, the •OH + Br^- reaction would yield the reactive radical $Br_2^{\bullet-}$[53], which might also be involved in BPA degradation. The additional reactions would be the following:

$$^{\bullet}OH + Br^- \rightarrow OH^- + Br^{\bullet} \quad (13)$$

$$^3CDOM* + Br^- \rightarrow CDOM^{\bullet-} + Br^{\bullet} \quad (14)$$

$$Br^- + Br^{\bullet} \rightarrow Br_2^{\bullet-} \quad (15)$$

$$2\ Br_2^{\bullet-} \rightarrow Br_2 + 2\ Br^- \quad (16)$$

$$Br_2^{\bullet-} + NO_2^- \rightarrow {}^{\bullet}NO_2 + 2\ Br^- \quad (17)$$

$$Br_2^{\bullet-} + DOM \rightarrow DOM^{\bullet+} + 2\ Br^- (DOM - Br + Br^-) \quad (18)$$

$$Br_2^{\bullet-} + BPA \rightarrow Products'' \quad (19)$$

where $k_{13} = 1.1\times10^{10}$ M^{-1} s^{-1}, $k_{14} = 3\times10^{9}$ M^{-1} s^{-1}, $k_{16} = 2\times10^{9}$ M^{-1} s^{-1}, $k_{17} = 2\times10^{7}$ M^{-1} s^{-1}, and $k_{18} = 306$ L mg$_C^{-1}$ s^{-1} [55]. As mentioned above $k_{19} = 2.5\times10^{8}$ M^{-1} s^{-1} was measured here by laser flash photolysis.

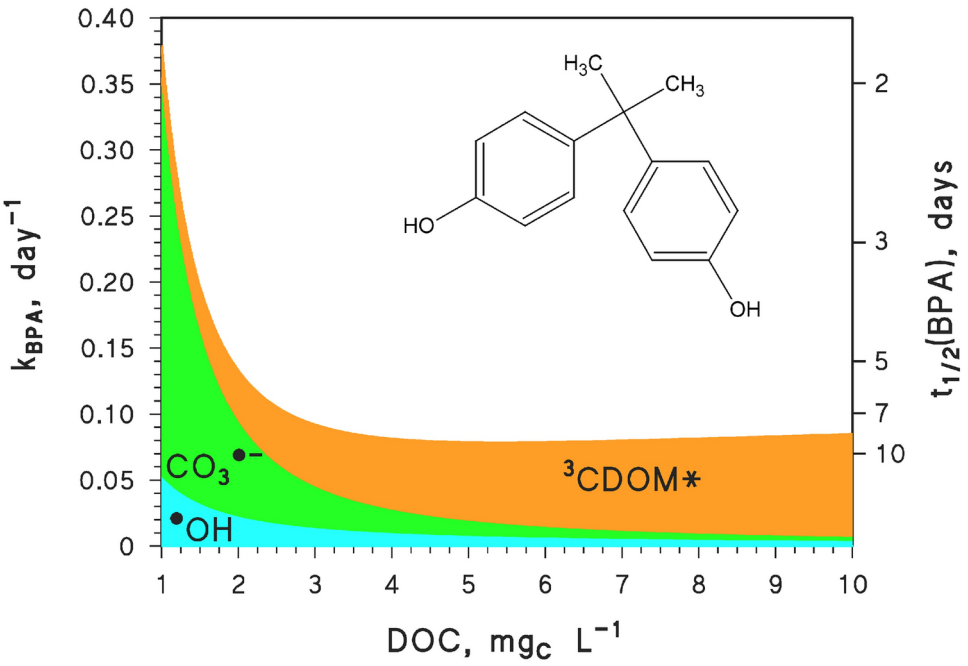

Fig. 1. Modeled photodegradation kinetics of BPA in freshwaters, as a function of the DOC. Other conditions: 3 m depth, 10^{-4} M NO_3^-, 10^{-6} M NO_2^-, 10^{-3} M HCO_3^-, 10^{-5} M CO_3^{2-}; sunlight irradiance as per fair-weather July at mid latitude.

When applying the steady-state approximation to both Br$^{\bullet}$ and $Br_2^{\bullet-}$ the following equations for, respectively, $Br_2^{\bullet-}$ formation rate, its steady-state concentration[55], and the pseudo-first order rate coefficient of BPA degradation by $Br_2^{\bullet-}$ are obtained:

$$R_{Br_2^{\cdot-}} = [Br^-]\,(k_{13}[^{\cdot}OH] + k_{14}[^3CDOM*]) \tag{20}$$

$$[Br_2^{\cdot-}] = \frac{-(k_{18}\,DOC + k_{17}[NO_2^-]) + \sqrt{(k_{18}\,DOC + k_{17}[NO_2^-])^2 + 4\,k_{16}\,R_{Br_2^{\cdot-}}}}{2\,k_{16}} \tag{21}$$

$$k_{BPA}^{Br_2^{\cdot-}} = k_{19}\,[Br_2^{\cdot-}] \tag{22}$$

The effect of the overall processes on BPA photodegradation is shown in Fig. 2. For sake of easier comparison, this figure represents identical conditions to Fig. 1 except for the 1 mM bromide concentration as per seawater chemistry. Figure 2, compared with Fig. 1, shows that the scavenging of $^{\bullet}$OH by Br^- almost totally suppresses the hydroxyl radical reaction and considerably inhibits $CO_3^{\bullet-}$-induced degradation as well.

The reason why the $CO_3^{\bullet-}$ process is not quenched as effectively as $^{\bullet}$OH is that part of $CO_3^{\bullet-}$ formation occurs upon CO_3^{2-} oxidation by ^{3}CDOM*:[54]

$$CO_3^{2-} + {}^3\,CDOM* \rightarrow CO_3^{\cdot-} + CDOM^{\cdot-} \tag{23}$$

At the same time, the reaction between BPA and $Br_2^{\bullet-}$ only plays minor role in overall degradation and is clearly unable to offset the inhibition of the $^{\bullet}$OH/$CO_3^{\bullet-}$ reactions. In this framework BPA degradation would be dominated by $CO_3^{\bullet-}$ at low DOC, and by ^{3}CDOM* for DOC > 2 $mg_C\ L^{-1}$.

So far we have not considered a possible role of $Cl_2^{\bullet-}$ (a reactive radical formed upon chloride oxidation)[52] in BPA degradation, but it would be most likely comparable to that of $Br_2^{\bullet-}$ and equally minor. Actually, chloride oxidation by $^{\bullet}$OH takes place at acidic pH[52] but it is poorly effective at the pH values of seawater[56], which thus inhibits a potentially important $Cl_2^{\bullet-}$ formation pathway that would be similar to that of $Br_2^{\bullet-}$ in reactions (13,15). As far as chloride oxidation by the excited states of photosensitizers is concerned, on average it is a couple of orders of magnitude slower compared to the oxidation of bromide[55,57]. Furthermore, there is indication that that the scavenging rate constant of $Cl_2^{\bullet-}$ by phenolic compounds that are representative of the antioxidant moieties of DOM is an order of magnitude faster than the scavenging rate constant of $Br_2^{\bullet-}$ [57,58]. Slower $Cl_2^{\bullet-}$ formation and faster scavenging compared to $Br_2^{\bullet-}$ would approximately offset the higher concentration of chloride compared to bromide in seawater, also considering that the second order reaction rate constant between $Cl_2^{\bullet-}$ and BPA is only around twice higher[59] compared to k_{19} between BPA and $Br_2^{\bullet-}$.

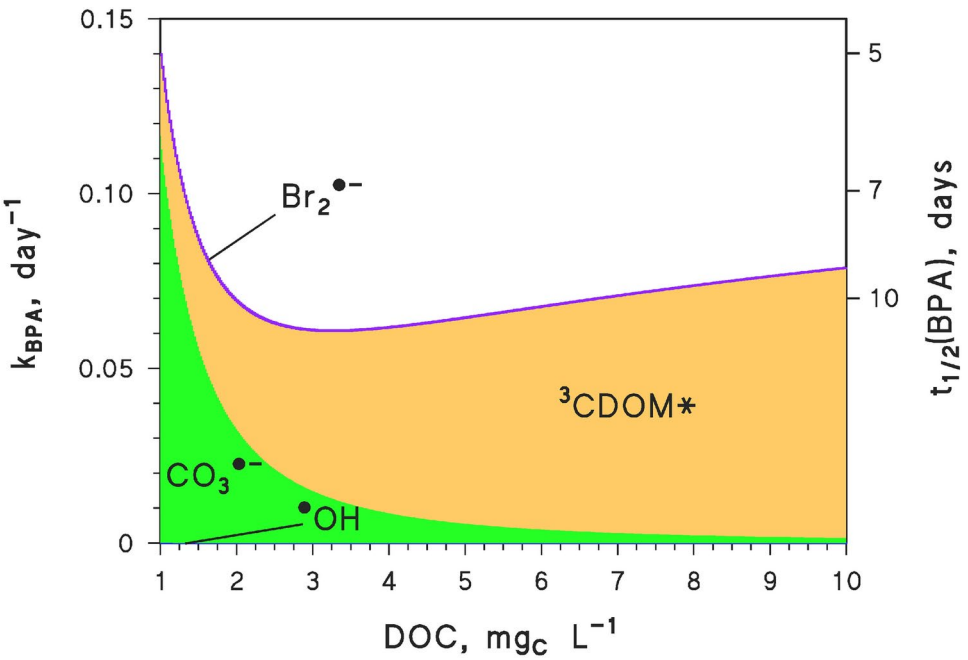

Fig. 2. Modeled photodegradation kinetics of BPA as a function of the DOC. Other conditions: 3 m depth, 10^{-4} M NO_3^-, 10^{-6} M NO_2^-, 10^{-3} M HCO_3^-, 10^{-5} M CO_3^{2-}, and 10^{-3} M Br^- (the latter as per seawater conditions); sunlight irradiance as per fair-weather July at mid latitude.

It should be noted that a recent study has found significant acceleration of •OH-induced BPA degradation upon addition of chloride[24]. However, the authors of the mentioned study have operated in the presence of 75% methanol, which scavenges •OH much more effectively than it scavenges $Cl_2^{\bullet-}$ [52,58]. Actually, in an organic phase containing excess methanol $Cl_2^{\bullet-}$ reactions would out-compete those with •OH[60]. However, their analysis was conducted in the aerosol phase of 100 nm particles and methanol is expected to evaporate completely before the BPA particles reacted heterogeneously with OH. The interpretation above would only hold if residual methanol were present in their particles.

As mentioned above, except for Br^- concentration, other conditions were kept the same in Figs. 1, 2 to make comparisons easier. Actually, despite considerable environmental variability, seawater is likely to contain lower values of nitrate, nitrite, as well as DOC compared to most freshwaters[61]. On the one hand, nitrate and nitrite produce •OH and enhance BPA degradation as a consequence, either directly through •OH reaction or indirectly via •OH-derived species such as $CO_3^{\bullet-}$. On the other hand, BPA degradation would usually be faster in low-DOC waters compared to high-DOC ones (see Figs. 1,2). There would thus be compensation between the prevailing freshwater and seawater conditions for NO_3^-, NO_2^- and DOC, as far as BPA photodegradation is concerned, with Br^- levels in seawater likely making most of the difference.

Interestingly, by considering the results reported in Figs. 1, 2 and despite the bromide effect, BPA photodegradation has potential to be slightly slower or about as fast as biodegradation[6] in freshwaters, but considerably faster than biodegradation in seawater. This means that seawater conditions could slow down biodegradation to a larger degree than they slow down photodegradation.

Product compounds detected by FT-ICR MS

Studies dedicated to the assessment of the product compounds formed by BPA degradation are scarce. Gas Chromatography Mass Spectrometry (GC–MS) coupled with derivatization technique has been used to detect and identify the product compounds formed by the photodegradation of BPA induced by fulvic acid[10]. Glycerol, 2-hydroxy-propanoic acid and p-hydroquinone have been identified by comparison with the mass spectra of authentic standards[10].

In the past two decades of research, FT-ICR-MS has been recognized as one of the most powerful analytical tools for the characterization of complex organic mixtures generated during chemical reactions[26,27,29,62–67]. Here, for the first time, we assess the complex product compounds formed by photosensitized degradation of BPA induced by ^{3}4-CB*. The FT-ICR-MS analysis of the product compounds generated by irradiation of 4-CB and 4-CB/BPA was here performed in the negative ion mode. Negative electrospray ionization mode (ESI-) was employed to achieve ionization of polar compounds as deprotonated molecules, $[M–H]^-$, without significant fragmentation. It has to be noted that BPA does not absorb light in the actinic region ($\lambda > 300$ nm) and, hence no direct photodegradation products would be formed. It should also be noted that, for each elemental composition assigned, multiple structural isomers are plausible[27,68,69]. Therefore, the same molecular formula can correspond to different compounds and the detected total number of CHO compounds is likely underestimated.

The relative abundances of the measured ions upon 2 h of irradiation of 4-CB and 4-CB/BPA are shown in Fig. 3A, B, respectively. The complexity of the product molecular composition markedly increased upon irradiation of the 4-CB/BPA mixture compared to 4-CB alone (see Fig. 3B and compare with Fig. 3A). Indeed, 226 CHO compounds were detected in ESI^- mode during the light irradiation of 4-CB at fixed pH 7.

When the aqueous mixture of 4-CB and BPA was irradiated for a time period of 2 h, then the number of CHO product compounds detected in ESI^- mode increased to 379 (Fig. 3B). Compared to 4-CB alone, the following new abundant peaks arose after 2 h of irradiation of 4-CB/BPA: *m/z* 215.10772, 227.20164, 239.12887, 257.08192, 273.11322, 319.13394, 333.11319, 357.20709, 371.22274, 377.17581, 467.14990, and 469.16555. These complex species most likely correspond to polyaromatic compounds and long-chain unsaturated compounds (vide infra).

The low average H/C (1.49) and O/C (0.34) ratios of the detected CHO compounds upon irradiation of 4-CB indicate their unsaturated characteristics[29,70]. The light irradiation of 4-CB/BPA yielded CHO compounds with even lower H/C (1.35) and O/C (0.32) ratios, suggesting that they are somewhat less saturated and less oxidized.

This observation was complemented by means of van Krevelen (VK) diagrams, in the form of H/C *versus* O/C ratios (Fig. 4). The VK plot can provide an estimate of the chemical characteristics of the many reaction products identified by FT-ICR-MS[68,69].

Based on H/C and O/C ratios, the detected CHO compounds are separated into two different regions, highlighted by red and green rectangles. The detected products in the red rectangle have high H/C ratio (≥ 1.5), and low O/C ratio < 0.5. These data suggest that they may be aliphatic CHO compounds[33,70]. Their number increased drastically from 82 during irradiation of 4-CB (red rectangle, Fig. 4A) to 98 during the photosensitized degradation of BPA by ^{3}4-CB* (red rectangle, Fig. 4B).

The aligned 33 compounds (blue rectangle) in Fig. 4A, with $H/C = 2$ and $DBE = 1$, are most likely aliphatic compounds such as alkanes, alkenes, and cyclic compounds[70]. Figure 4B shows that the photosensitized chemistry of BPA by ^{3}4-CB* leads to a slight increase of these aliphatic compounds to 36 (blue rectangle). It is reasonable that generation of such species is triggered by reductive processes such as Eq. (5), or corresponding reactions that involve ^{3}4-CB* + 4-CB. The formation of $4\text{-CB}^{\bullet-}$ would be enhanced in the presence of BPA.

The CHO compounds in the green rectangle have molecular formulas with low H/C (≤ 1.0) and low O/C (≤ 0.5) ratios, suggesting a degree of unsaturation that represents the number of rings plus the number of double bonds, plus twice the number of triple bonds[71] (Fig. 4A, B). Therefore, these compounds should contain one or more aromatic rings. High degrees of unsaturation, with DBE values ranging between 5 and 20, include 29 chemical formulas depicted in the green rectangle (Fig. 4A). In the case of irradiation of BPA/4-CB, these compounds increased to 92 (Fig. 4B). DBE values of up to 20 (green rectangle in Fig. 4B) suggest the formation of oligomers[62,63] and polyaromatic compounds. The regular addition of the CH_2 repeating increments is partly responsible for the increase in both the molecular mass, and DBE values[26,62,64] (Fig. 4).

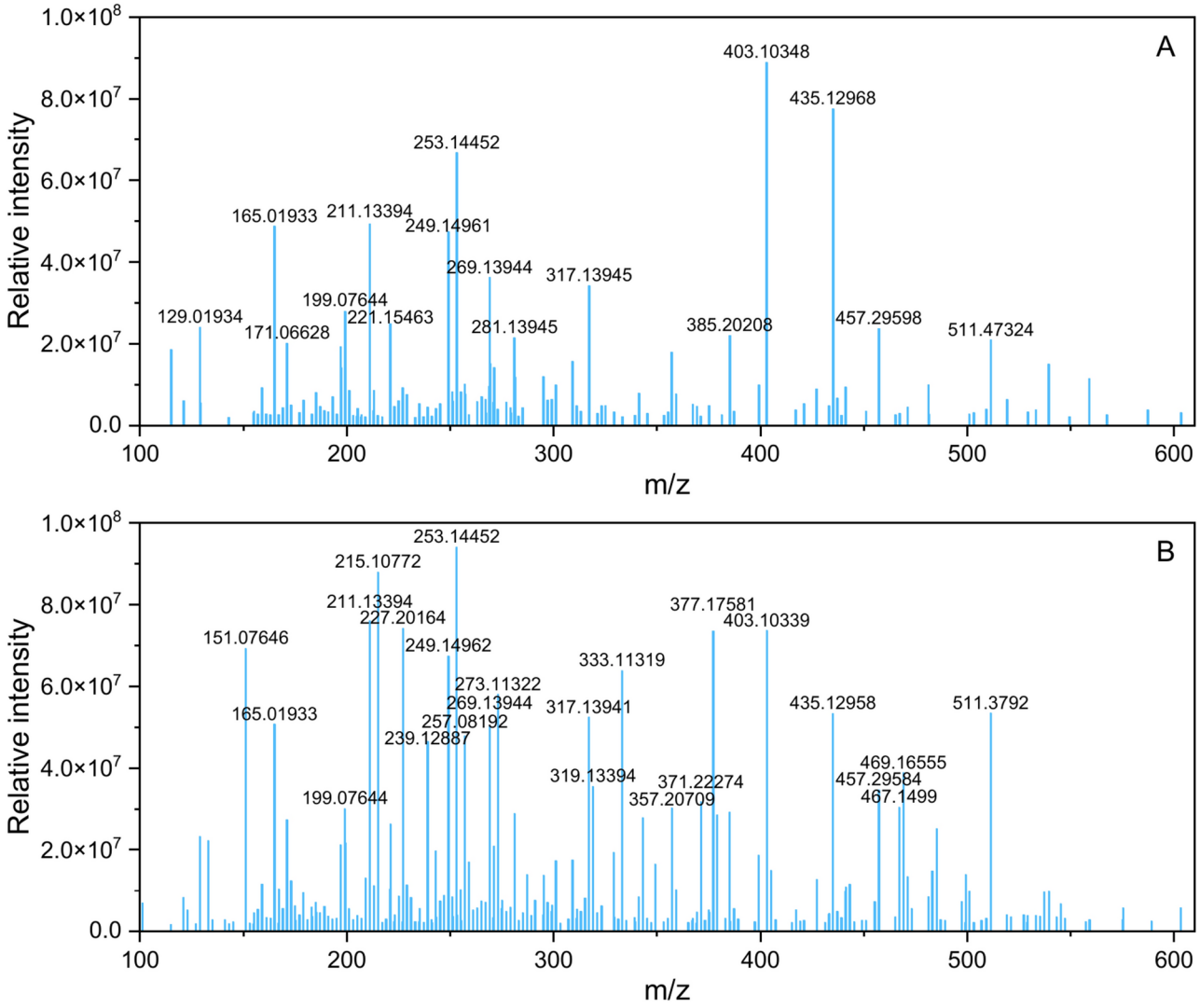

Fig. 3. Comparison of relative abundances scanned in ESI- mode between (**A**) 10^{-5} M 4-CB after 2 h irradiation; (**B**) mixture of 10^{-5} M 4-CB and 10^{-5} M BPA after 2 h irradiation.

Aromatic properties of the CHO product compounds were further examined by the use of the aromaticity equivalent (X_c) (Eq. 1). According to this parameter the detected compounds are divided in three groups: aliphatic compounds ($X_c < 2.5$), aromatic compounds with a benzene core structure ($2.5 \leq X_c < 2.7$), and polyaromatic compounds ($X_c \geq 2.7$)[32–34]. During the photosensitized degradation of BPA by ^{3}4-CB*, there were 97 polyaromatic compounds ($X_c \geq 2.7$), in reasonable agreement with the DBE values analysis. Actually, triplet sensitized oxidation of a phenolic compound like BPA is expected to produce phenoxy radicals, which are prone to dimerization and oligomerization processes[20] that could well yield high-molecular weight compounds with high DBE and $X_c \geq 2.7$.

Photosensitized degradation of BPA by ^{3}4-CB* in the presence of inorganic salts

Photosensitized degradation of BPA by ^{3}4-CB* was also studied by adding 0.7 M NaCl and 1×10^{-3} M NaBr as per seawater conditions. The presence of inorganic ions additionally increased the complexity of the observed CHO product compounds (Fig. 4C,D). In the presence of inorganic salts, the number of aliphatic and benzene-like compounds (red rectangles) decreased to 51 and 74 during the light irradiation of 4-CB and 4-CB/BPA, respectively. In contrast, the number of unsaturated compounds with DBE values ranging between 6 and 20 and of polyaromatic compounds largely increased to 50 and 136, respectively, upon irradiation of 4-CB and 4-CB/BPA (green rectangles).

The relative abundances of the compounds measured after 2 h of irradiation of 4-CB and 4-CB/BPA in the presence of salts are shown in Supplementary Fig. S4. The number of detected CHO compounds arising from 4-CB irradiation was similar with (216) and without (226) inorganic salts. In contrast, in the case of 4-CB/BPA irradiation, salt addition caused a notable increase, from 379 to 423, of the detected compounds number.

The addition of salts also altered the prevailing chemical structures. Indeed, the average H/C ratio of compounds detected upon 4-CB irradiation with salts, compared to no-salt irradiation, decreased to 1.3 (i.e.,

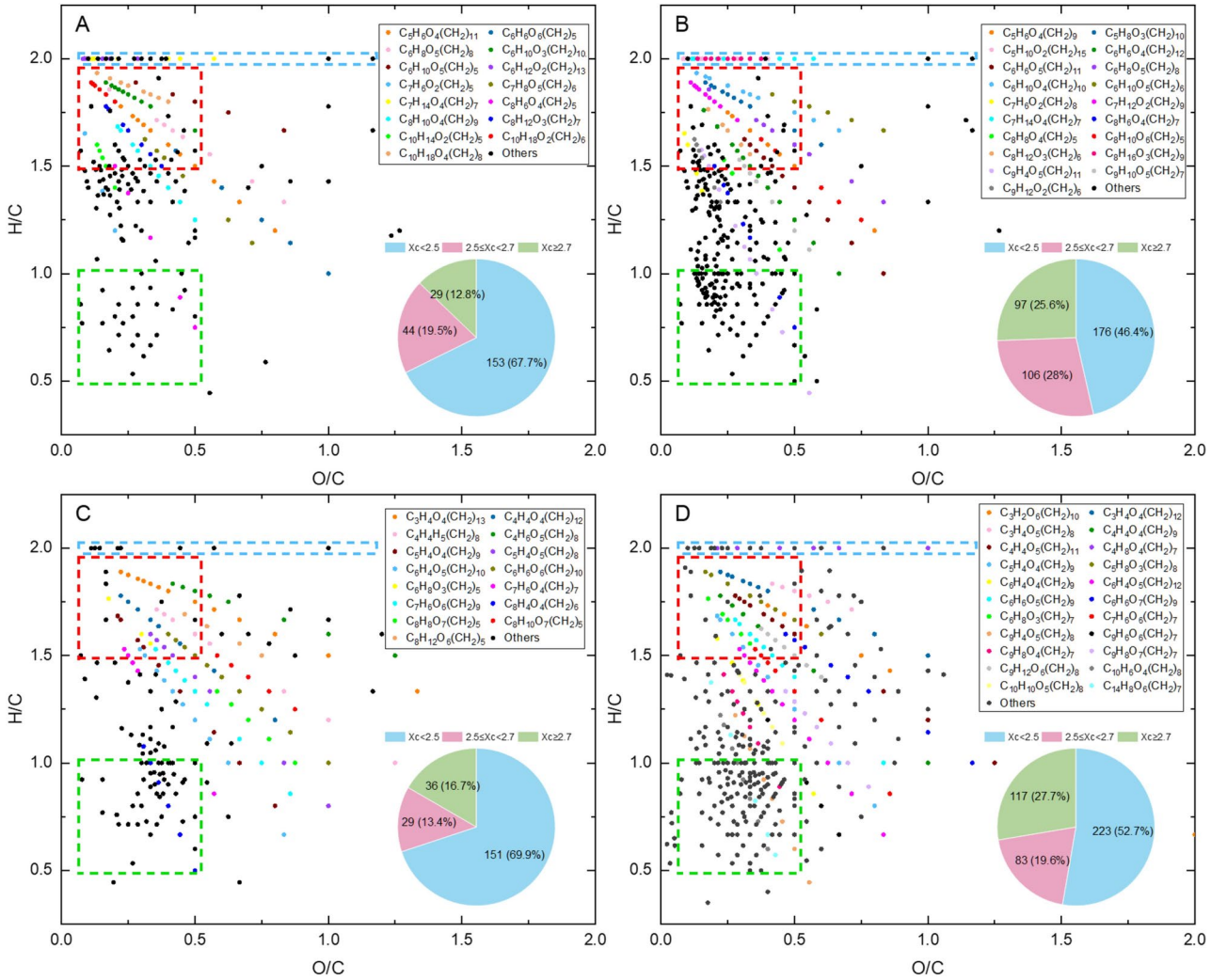

Fig. 4. The van Krevelen plots of CHO compounds formed upon light irradiation of: (**A**) 4-CB; (**B**) 4-CB/BPA; (**C**) 4-CB in the presence of 0.7 M NaCl and 1×10^{-3} M NaBr; (**D**) 4-CB/BPA in the presence of 0.7 M NaCl and 1×10^{-3} M NaBr. Pie charts show the percentage value and number of compounds of each color-coded group in the sample according to the aromaticity equivalent parameter (blue with $Xc < 2.5$, red with $2.5 \leq Xc < 2.7$, and green with $Xc \geq 2.7$). Regular additions of CH_2 repeating increments in molecular subunits are also shown.

more unsaturated compounds) while O/C increased to 0.48 (slight increase of oxygenation). In the case of 4-CB/BPA irradiation in the presence of inorganic salts the values of H/C (1.22) and O/C (0.42) were even lower, suggesting an increase of polyaromatic and unsaturated compounds. In this framework, it has to be noted that the SPE procedure may not retain well some low-molecular weight CHO compounds such as carboxylic acids, which usually have $O/C > 1$. Therefore, actual O/C ratios of compounds produced by BPA and 4-CB may be somewhat higher than found here.

The enhancement of polyaromatic compounds formation in the presence of seawater salts might be due to the fact that Br^- reacts with ^{3}4-CB* that would otherwise be quenched by O_2, to finally yield $Br_2^{\bullet-}$ that is a one-electron oxidant[55] and could oxidize BPA to its phenoxy radical, which enhances oligomerization. Interestingly, no Cl- or Br-containing compounds were detected, implying that BPA oligomerization would prevail over halogenation. In laboratory conditions there would be no $Br_2^{\bullet-}$ scavengers other than BPA or 4-CB, which would account for the observed salt effect. In the natural environment $Br_2^{\bullet-}$ would be largely scavenged by DOM, thereby inhibiting its reaction with BPA that would thus be minor, as shown in Fig. 2. Similar reactions as those discussed for $Br^-/Br_2^{\bullet-}$ might involve $Cl^-/Cl_2^{\bullet-}$, in both laboratory conditions and the natural environment.

Interestingly, compared to freshwater conditions (Fig. 1) and especially at low DOC, seawater salts would shift BPA degradation away from the hydroxylating agent $^{\bullet}OH$ to one-electron oxidants such as $CO_3^{\bullet-}$ and ^{3}CDOM* (Fig. 2). In this case as well, phenoxy radical formation triggered by one-electron oxidants (but not or poorly by $^{\bullet}OH$)[17,40] would favor oligomer formation.

Environmental implications

The results shown here indicate that an emerging contaminant as BPA can be efficiently removed by photosensitized reactions initiated by 4-CB, used as CDOM proxy in conditions that simulated either freshwaters, or the SML and liquid water of marine aerosols. Interestingly, BPA photodegradation and biodegradation kinetics could be comparable in sunlit freshwaters. In contrast, the photodegradation of BPA in the seawater, albeit slower than in the case of freshwaters, has potential to proceed faster than seawater biodegradation. In other words, the different conditions of seawater (salinity, biota) compared to freshwater would inhibit biodegradation much more than photodegradation. Furthermore, the presence of inorganic salts (NaCl + NaBr) yielded fewer monoaromatic compounds from BPA sensitized degradation, but largely increased the number of oligomers and polyaromatic compounds. Therefore, there would be potential for the latter to be formed in higher amount in SML and in the liquid water of marine aerosols than in freshwaters and/or dilute cloud-water. Considering that polyaromatic compounds may absorb solar actinic radiation, our results suggest that NaCl/NaBr could alter photosensitized chemistry and consequently modify the light-absorbing properties of marine aerosols, which play a role in the Earth's radiative balance.

Data availability

All data generated or analyzed during this study are included in this published article and its supplementary information files.

Received: 1 June 2024; Accepted: 9 December 2024
Published online: 30 December 2024

References

1. Wright, S. L. & Kelly, F. J. Plastic and human health: A micro issue?. *Environ. Sci. Technol.* **51**, 6634–6647 (2017).
2. Jambeck, J. R. et al. Plastic waste inputs from land into the ocean. *Science.* **347**, 768–771 (2015).
3. Bhatnagar, A. & Anastopoulos, L. Adsorptive removal of bisphenol A (BPA) from aqueous solution: A review. *Chemosphere.* **168**, 885–902 (2017).
4. Alonso-Magdalena, P. et al. Bisphenol-A acts as a potent estrogen via non-classical estrogen triggered pathways. *Mol. Cell. Endocrinol.* **355**, 201–207 (2012).
5. Shehab, Z. N., Jamil, N. R. & Aris, A. Z. Occurrence, environmental implications and risk assessment of Bisphenol A in association with colloidal particles in an urban tropical river in Malaysia. *Sci. Rep*. **10** (2020).
6. Im, J. & Loffler, F. E. Fate of bisphenol A in terrestrial and aquatic environments. *Environ. Sci. Technol.* **50**, 8403–8416 (2016).
7. Ying, G. G. & Kookana, R. S. Degradation of five selected endocrine-disrupting chemicals in seawater and marine sediment. *Environ. Sci. Technol.* **37**, 1256–1260 (2003).
8. Chin, Y. P., Miller, P. L., Zeng, L. K., Cawley, K. & Weavers, L. K. Photosensitized degradation of bisphenol a by dissolved organic matter. *Environ. Sci. Technol.* **38**, 5888–5894 (2004).
9. Deborde, M., Rabouan, S., Mazellier, P., Duguet, J.-P. & Legube, B. Oxidation of bisphenol A by ozone in aqueous solution. *Water Res.* **42**, 4299–4308 (2008).
10. Zhan, M. J., Yang, X., Xian, Q. M. & Kong, L. G. Photosensitized degradation of bisphenol A involving reactive oxygen species in the presence of humic substances. *Chemosphere.* **63**, 378–386 (2006).
11. Wang, B., Wu, F., Li, P. & Deng, N. UV-light induced photodegradation of bisphenol a in water: Kinetics and influencing factors. *React. Kinetics Catal. Lett.* **92**, 3–9 (2007).
12. Peng, Z., Wu, F. & Deng, N. S. Photodegradation of bisphenol A in simulated lake water containing algae, humic acid and ferric ions. *Environ. Pollut.* **144**, 840–846 (2006).
13. Tsui, M. M. P. et al. Occurrence, distribution and ecological risk assessment of multiple classes of UV filters in surface waters from different countries. *Water Res.* **67**, 55–65 (2014).
14. Vione, D. et al. Photochemical reactions in the tropospheric aqueous phase and on particulate matter. *Chem. Soc. Rev.* **35**, 441–453 (2006).
15. Gomez Alvarez, E., Wortham, H., Strekowski, R., Zetzsch, C. & Gligorovski, S. Atmospheric photosensitized heterogeneous and multiphase reactions: From outdoors to indoors. *Environ. Sci. Technol.* **46**, 1955-1963 (2012).
16. Simoneit, B. R. Aqueous high-temperature and high-pressure organic geochemistry of hydrothermal vent systems. *Geochim. Cosmochim. Acta.* **57**, 3231–3243 (1993).
17. Jang, M. & McDow, S. R. Benz a anthracene photodegradation in the presence of known organic constituents of atmospheric aerosols. *Environ. Sci. Technol.* **29**, 2654–2660 (1995).
18. Jang, M. & McDow, S. R. Products of benz a anthracene photodegradation in the presence of known organic constituents of atmospheric aerosols. *Environ. Sci. Technol.* **31**, 1046–1053 (1997).
19. Anastasio, C., Faust, B. C. & Rao, C. J. Aromatic carbonyl compounds as aqueous-phase photochemical sources of hydrogen peroxide in acidic sulfate aerosols, fogs, and clouds .1. Non-phenolic methoxybenzaldehydes and methoxyacetophenones with reductants (phenols). *Environ. Sci. Technol.* **31**, 218–232 (1997).
20. De Laurentiis, E. et al. Could triplet-sensitised transformation of phenolic compounds represent a source of fulvic-like substances in natural waters?. *Chemosphere.* **90**, 881–884 (2013).
21. Canonica, S., Hellrung, B. & Wirz, J. Oxidation of phenols by triplet aromatic ketones in aqueous solution. *J. Phys. Chem. A.* **104**, 1226–1232 (2000).
22. Smith, J. D., Sio, V., Yu, L., Zhang, Q. & Anastasio, C. Secondary organic aerosol production from aqueous reactions of atmospheric phenols with an organic triplet excited state. *Environ. Sci. Technol.* **48**, 1049–1057 (2014).
23. Jammoul, A., Gligorovski, S., George, C. & D'Anna, B. Photosensitized heterogeneous chemistry of ozone on organic films. *J. Phys. Chem. A* **112**, 1268–1276 (2008).
24. Kruse, S. M. & Slade, J. H. Heterogeneous and photosensitized oxidative degradation kinetics of the plastic additive bisphenol-A in sea spray aerosol mimics. *J. Phys. Chem. A.* **127**, 4724–4733 (2023).
25. Loisel, G. *et al.* Ionic strength effect on the formation of organonitrate compounds through photochemical degradation of vanillin in liquid water of aerosols. *Atmos. Environ.* **246** (2021).
26. Wang, Y. et al. Ionic strength effect triggers brown carbon formation through heterogeneous ozone processing of ortho-vanillin. *Environ. Sci. Technol.* **55**, 4553–4564 (2021).
27. Bianco, A. et al. Chemical characterization of cloudwater collected at Puy de Dome by FT-ICR MS reveals the presence of SOA components. *ACS Earth Sp. Chem.* **3**, 2076–2087 (2019).
28. LeClair, J. P., Collett, J. L. & Mazzoleni, L. R. Fragmentation analysis of water-soluble atmospheric organic matter using ultrahigh-resolution FT-ICR mass spectrometry. *Environ. Sci. Technol.* **46**, 4312–4322 (2012).

29. Zhao, Y., Hallar, A. G. & Mazzoleni, L. R. Atmospheric organic matter in clouds: exact masses and molecular formula identification using ultrahigh-resolution FT-ICR mass spectrometry. *Atmos. Chem. Phys.* **13**, 12343–12362 (2013).
30. Shi, Q. *et al.* Characterization of middle-temperature gasification coal tar. Part 3: Molecular composition of acidic compounds. *Energy Fuels* **27**, 108-117 (2013).
31. Jiang, B. et al. Polycyclic aromatic hydrocarbons (PAHs) in ambient aerosols from Beijing: Characterization of low volatile PAHs by positive-ion atmospheric pressure photoionization (APPI) coupled with Fourier transform ion cyclotron resonance. *Environ. Sci. Technol.* **48**, 4716–4723 (2014).
32. Yassine, M. M., Harir, M., Dabek-Zlotorzynska, E. & Schmitt-Kopplin, P. Structural characterization of organic aerosol using Fourier transform ion cyclotron resonance mass spectrometry: Aromaticity equivalent approach. *Rapid Commun. Mass Spectrom.* **28**, 2445–2454 (2014).
33. Kourtchev, I. et al. Molecular composition of organic aerosols in central Amazonia: An ultra-high-resolution mass spectrometry study. *Atmos. Chem. Phys.* **16**, 11899–11913 (2016).
34. Wang, X. et al. Chemical characteristics of organic aerosols in Shanghai: A study by ultrahigh-performance liquid chromatography coupled with orbitrap mass spectrometry. *J. Geophys. Res. Atmos.* **122**, 11703–11722 (2017).
35. Fabbri, D. *et al.* Assessing the photodegradation potential of compounds derived from the photoinduced weathering of polystyrene in water. *Sci. Total Environ.* **876** (2023).
36. Minella, M. et al. An experimental methodology to measure the reaction rate constants of processes sensitised by the triplet state of 4-carboxybenzophenone as a proxy of the triplet states of chromophoric dissolved organic matter, under steady-state irradiation conditions. *Environ. Sci. Process Impacts.* **20**, 1007–1019 (2018).
37. Marciniak, B., Bobrowski, K., Hug, G. L. & Rozwadowski, J. Photoinduced electron transfer between sulfur-containing carboxylic acids and the 4-carboxybenzophenone triplet state in aqueous solution. *J. Phys. Chem. C.* **98**, 4854–4860 (1994).
38. McNeill, K. & Canonica, S. Triplet state dissolved organic matter in aquatic photochemistry: Reaction mechanisms, substrate scope, and photophysical properties. *Environ. Sci. Process Impacts.* **18**, 1381–1399 (2016).
39. Luo, Z. H. *et al.* Environmental implications of superoxide radicals: From natural processes to engineering applications. *Water Res.* **261** (2024).
40. Bedini, A. et al. Phototransformation of anthraquinone-2-sulphonate in aqueous solution. *Photochem. Photobiol. Sci.* **11**, 1445–1453 (2012).
41. Carena, L., Puscasu, C. G., Comis, S., Sarakha, M. & Vione, D. Environmental photodegradation of emerging contaminants: A re-examination of the importance of triplet-sensitised processes, based on the use of 4-carboxybenzophenone as proxy for the chromophoric dissolved organic matter. *Chemosphere.* **237** (2019).
42. Lee, J., von Gunten, U. & Kim, J.-H. Persulfate-based advanced oxidation: Critical assessment of opportunities and roadblocks. *Environ. Sci. Technol.* **54**, 3064–3081 (2020).
43. Wilkinson, F., Helman, W. P. & Ross, A. B. Rate constants for the decay and reactions of the lowest electronically excited singlet state of molecular oxygen in solution. An expanded and revised compilation. *J. Phys. Chem. Ref. Data* **24**, 663–677 (1995).
44. Wenk, J., von Gunten, U. & Canonica, S. Effect of dissolved organic matter on the transformation of contaminants induced by excited triplet states and the hydroxyl radical. *Environ. Sci. Technol.* **45**, 1334–1340 (2011).
45. Wenk, J. & Canonica, S. Phenolic antioxidants inhibit the triplet-induced transformation of anilines and sulfonamide antibiotics in aqueous solution. *Environ. Sci. Technol.* **46**, 5455–5462 (2012).
46. Carena, L., Vione, D., Minella, M., Canonica, S. & Schoenenberger, U. Inhibition by phenolic antioxidants of the degradation of aromatic amines and sulfadiazine by the carbonate radical ($CO_3^{\bullet-}$). *Water Res.* **209** (2022).
47. Vione, D. A critical view of the application of the APEX software (aqueous photochemistry of environmentally-occurring xenobiotics) to predict photoreaction kinetics in surface freshwaters. *Molecules.* **25** (2020).
48. Estimation programs interface suite™ for Microsoft® windows, v 4.11 (United States Environmental Protection Agency, Washington, DC, USA, 2012).
49. Peller, J. R., Mezyk, S. P. & Cooper, W. J. Bisphenol A reactions with hydroxyl radicals: diverse pathways determined between deionized water and tertiary treated wastewater solutions. *Res. Chem. Intermed.* **35**, 21–34 (2009).
50. Sanchez-Polo, M., Daiem, M. M. A., Ocampo-Perez, R., Rivera-Utrilla, J. & Mota, A. J. Comparative study of the photodegradation of bisphenol A by HO·, $SO_4^{\bullet-}$ and $CO_3^{\bullet-}$/HCO_3· radicals in aqueous phase. *Sci. Total Environ.* **463**, 423–431 (2013).
51. Wang, L., Xiao, K. & Zhao, H. The debatable role of singlet oxygen in persulfate-based advanced oxidation processes. *Water Res.* **235** (2023).
52. Buxton, G. V., Greenstock, C. L., Helman, W. P. & Ross, A. B. Critical Review of rate constants for reactions of hydrated electrons, hydrogen atoms and hydroxyl radicals (·OH/·O^- in aqueous solution). *J. Phys. Chem. Ref. Data* **17**, 513–886 (1988).
53. Parker, K. M. & Mitch, W. A. Halogen radicals contribute to photooxidation in coastal and estuarine waters. *Proc. Natl. Acad. Sci. U.S.A.* **113**, 5868–5873 (2016).
54. Canonica, S. et al. Photosensitizer method to determine rate constants for the reaction of carbonate radical with organic compounds. *Environ. Sci. Technol.* **39**, 9182–9188 (2005).
55. De Laurentiis, E. et al. Assessing the occurrence of the dibromide radical ($Br^{2-}\bullet$) in natural waters: Measures of triplet-sensitised formation, reactivity, and modelling. *Sci. Total Environ.* **439**, 299–306 (2012).
56. Vione, D. et al. Sources and sinks of hydroxyl radicals upon irradiation of natural water samples. *Environ. Sci. Technol.* **40**, 3775–3781 (2006).
57. Brigante, M. et al. Formation and reactivity of the dichloride radical (Cl_2^-) in surface waters: A modelling approach. *Chemosphere.* **95**, 464–469 (2014).
58. Neta, P., Huie, R. E. & Ross, A. B. Rate constants for reactions of inorganic radicals in aqueous solution. *J. Phys. Chem. Ref. Data.* **17**, 1027–1284 (1988).
59. Song, Z. *et al.* Kinetics and mechanisms of non-radically and radically induced degradation of bisphenol A in a peroxymonosulfate-chloride system. *Environ. Sci. Ecotechnol.* **22** (2024).
60. Coha, M., Farinelli, G., Tiraferri, A., Minella, M. & Vione, D. Advanced oxidation processes in the removal of organic substances from produced water: Potential, configurations, and research needs. *Chem. Eng. J.* **414** (2021).
61. Granskog, M. A., Kaartokallio, H., Thomas, D. N. & Kuosa, H. Influence of freshwater inflow on the inorganic nutrient and dissolved organic matter within coastal sea ice and underlying waters in the Gulf of Finland (Baltic Sea). *Estuarine Coastal Shelf Sci.* **65**, 109–122 (2005).
62. Altieri, K. E., Carlton, A. G., Lim, H.-J., Turpin, B. J. & Seitzinger, S. P. Evidence for oligomer formation in clouds: Reactions of isoprene oxidation products. *Environ. Sci. Technol.* **40**, 4956–4960 (2006).
63. Altieri, K. E. et al. Oligomers formed through in-cloud methylglyoxal reactions: Chemical composition, properties, and mechanisms investigated by ultra-high resolution FT-ICR mass spectrometry. *Atmos. Environ.* **42**, 1476–1490 (2008).
64. Mekic, M. et al. Ionic-strength effects on the reactive uptake of ozone on aqueous pyruvic acid: Implications for air-sea ozone deposition. *Environ. Sci. Technol.* **52**, 12306–12315 (2018).
65. Mekic, M. *et al.* Formation of highly oxygenated multifunctional compounds from cross-reactions of carbonyl compounds in the atmospheric aqueous phase. *Atmos. Environ.* **219** (2019).
66. Wang, Y. *et al.* Molecular characterization of the product compounds formed upon heterogeneous chemistry of ozone with riverine surface microlayer. *J. Geophys. Res. Atmos.* **127** (2022).

67. Li, P. *et al.* Impact of nitrate and iron ions on uptake coefficients and condensed phase products from the reaction of gaseous NO_2 with HULIS proxies. *J. Geophys. Res. Atmos.* **129** (2024).
68. Altieri, K. E., Turpin, B. J. & Seitzinger, S. P. Oligomers, organosulfates, and nitrooxy organosulfates in rainwater identified by ultra-high resolution electrospray ionization FT-ICR mass spectrometry. *Atmos. Chem. Phys.* **9**, 2533–2542 (2009).
69. Mazzoleni, L. R. et al. Identification of water-soluble organic carbon in non-urban aerosols using ultrahigh-resolution FT-ICR mass spectrometry: Organic anions. *Environ. Chem.* **9**, 285–297 (2012).
70. Wang, K., Zhang, Y., Huang, R.-J., Cao, J. & Hoffman, T. UHPLC-Orbitrap mass spectrometric characterization of organic aerosol from a central European city (Mainz, Germany) and a Chinese megacity (Beijing). *Atmos. Environ.* **189**, 22–29 (2018).
71. Pellegrin, V. Molecular formulas of organic compounds: the nitrogen rule and degree of unsaturation. *J. Chem. Educ.* **60**, 626 (1983).

Acknowledgements

This study was financially supported by National Natural Science Foundation of China, Research Fund for International Scientists (4221101064), National Natural Science Foundation of China (42177087), the Science Fund for Creative Research Groups of the National Natural Science Foundation of China (42321003), Ministry of Science and Technology of China (2022YFC3701102), and the Guangdong Foundation for Program of Science and Technology Research (2023B1212060049). DV and LC acknowledge financial support from the Project CH4.0 under the MUR program "Dipartimenti di Eccellenza 2023-2027" (CUP: D13C22003520001). DV also acknowledges support by MUR-PRIN 20227FS42S, project PHOTOPLAST (CUP: D53D23009020006).

Author contributions

Y.W.: Data curation, Formal analysis, Investigation, Methodology; Q. D.: Data curation, Formal analysis; Y.W.: Investigation, Methodology; P.L.: Formal analysis; B.J.: Investigation; J.L.: Investigation; P.C.: Formal analysis, Investigation; M.B.: Investigation, Visualization; D.D'A.: Formal analysis, Investigation; L.C.: Formal analysis, Data Curation; Investigation; H.C.: Visualization, Writing-Original draft, Supervision, Resources; D.V.: Writing-Original draft, Funding acquisition, Supervision; S.G.: Conceptualization, Supervision, Resources, Funding acquisition.

Additional information

Supplementary Information The online version contains supplementary material available at https://doi.org/10.1038/s41598-024-82865-y.

Correspondence and requests for materials should be addressed to H.C., D.V. or S.G.